

Free-electron-laser gain degradation and electron-beam quality

W. B. Colson

Berkeley Research Associates, Inc., P.O. Box 241, Berkeley, California 94701

J. C. Gallardo and P. M. Bosco

Quantum Institute, University of California, Santa Barbara, California 93106

(Received 1 May 1986)

The free-electron laser can be described by solving the Lorentz-Maxwell equations self-consistently in weak optical fields. The field evolution is determined by an integral equation that allows the inclusion of an arbitrary electron distribution function in a simple way. Contour maps are used to show the gain degradation due to an electron-beam energy spread and an electron-beam angular spread. In the limit of low gain, the gain spectrum is related to the spontaneous emission line shape through successively higher derivatives. In the limit of high gain, it is shown that the growth rate becomes less susceptible to degradation from the electron-beam quality.

I. INTRODUCTION

In a free-electron laser (FEL), a relativistic electron beam amplifies a copropagating, coherent optical wave traveling through a periodic undulator magnetic field.¹ In the oscillator configuration, coherent electron bunching develops on each pass while resonator mirrors allow the stored optical power to grow over many passes. In the amplifier configuration, coherent electron bunches develop rapidly in the first part of the undulator followed by rapid growth of the optical field. Maintaining the coherence of the electron bunches over a significant interaction length imposes important restrictions on the electron-beam quality. An energy or angular spread (due to emittance) contributes a random component to the electron motion that decreases the coherent bunching in time.

Some of the earliest FEL experiments used electron beams that were essentially monoenergetic,²⁻⁵ but practically all subsequent experiments have made use of higher current sources with significant energy spread or emittance. Many accelerators present a design trade off between high-current and high-beam quality. This makes it essential to accurately evaluate the effects of beam quality in present and future experiments. It is particularly important for FEL's designed to operate at extreme uv or x-ray wavelengths.⁶ Several theoretical models involving simulations and plasma dispersion relations have discussed the detrimental effects of electron-beam quality in the FEL interaction.⁷⁻²⁴ The theory presented here uses a convenient, yet powerful, method of including an arbitrary electron distribution function in a self-consistent integral equation for the complex optical field. FEL gain and the effects of beam quality can then be calculated analytically or integrated on a small computer.

Since the basic equations solved here are the same as in computer simulations or the plasma dispersion methods, specific physical results have been shown to agree with those methods when a direct comparison is possible. The computer simulations have proved to be a useful method of understanding many aspects of the FEL interaction,

but one of the most difficult effects to accurately characterize is that of electron-beam quality. Even a prohibitively large number of sample particles is far short of the number in a real experiment, and yet introduces a large amount of numerical noise when distributed over a large volume of phase space. To reproduce some of the results shown later in this paper, we found the simulation method to be several hundred to a thousand times less efficient. While many other FEL topics are most efficiently studied through simulations, the detrimental effects of beam quality are probably better handled through a combination of analytic and numerical techniques. The stability analysis used to obtain plasma dispersion relations usually calculates the reduced FEL growth rates due to poor beam quality. This method can lead to analytical expressions, but depends upon specific models for the electron-beam distribution, and does not easily describe more complicated transient behavior where the FEL growth rate is not constant; the FEL is often designed to operate in this regime. In addition, the exact formulation presented here works smoothly between different regimes of operation like high and low gain. The only requirement is weak optical fields.

II. BASIC THEORY

We solve the electron Lorentz and optical wave equations self-consistently with the assumption of weak optical fields. The effects of beam quality are typically less important when the optical field strength is large near saturation, and the issue of beam quality is most important in weak fields where the accurate evaluation of gain can determine whether the FEL is above or below threshold.

The electrons travel through a periodic undulator with the field on the z axis described by $\mathbf{B} = B[\cos(k_0 z), \sin(k_0 z), 0]$ where B is the peak magnetic field amplitude. The undulator field extends over a length $L = N\lambda_0$ with a number of periods N , and wavelength $\lambda_0 = 2\pi/k_0$. The electron velocity in a perfect helical orbit is

$$c\beta = c[-(K/\gamma)\cos(k_0z), -(K/\gamma)\sin(k_0z), \beta_0],$$

where $K = eB\lambda_0/2\pi mc^2$, e is the electron's charge magnitude, m is the electron's mass, c is the speed of light, $\beta_0 = [1 - (1 + K^2)/\gamma^2]^{1/2}$, and γmc^2 is the electron's energy. Imperfect injection due to poor beam quality is more meaningfully introduced after some further theoretical development. A typical undulator uses $B \approx 2$ kG and $\lambda_0 \approx 5$ cm, so that $K \approx 1$. Since the electrons are relativistic ($\gamma \gg 1$), the transverse excursions are small compared to λ_0 .

The optical vector potential with the polarization that best couples to the above trajectory is $\mathbf{A} = k^{-1} |E| [\sin\Psi, \cos\Psi, 0]$ where $\Psi = kz - \omega t + \phi$, and $\lambda = 2\pi/k = 2\pi c/\omega$ is the optical carrier wavelength. The complex electric field envelope, $E(z, t) = |E(z, t)| e^{i\phi(z, t)}$, is taken to vary slowly in z and t , so that terms containing two derivatives in the wave equation are small compared to terms with single derivatives.²⁵ No transverse (x, y) dependence is included so that diffraction is taken to be small over the interaction length L , and the electron beam remains aligned near the center of the optical mode. The transverse motion above, proportional to (K/γ) , defines the transverse current for each electron in the beam. If the current density is uniform over a sufficient length, each point $z + ct$ in the optical field envelope evolves according to the slowly varying wave equation²⁵

$$\frac{da}{d\tau} = -j \langle e^{-i\xi} \rangle, \quad (1)$$

where $a = 4N\pi eKLE/\gamma^2 mc^2$ is the dimensionless optical field strength, $\tau = ct/L$ is the dimensionless time ($0 \leq \tau \leq 1$), $j = 8N(\pi eKL)^2 \rho/\gamma^3 mc^2$ is the dimensionless current density, ρ is the actual electron particle density, $\xi = (k + k_0)z - \omega t$ is the electron phase in the combined optical and undulator fields, and $\langle \dots \rangle$ represents a normalized average over all electrons in the beam driving $a(\tau)$. The electrons are labeled by their initial phase-space coordinates; the initial phase is $\xi_i = \xi(0)$, and the initial phase velocity is

$$v_i = d\xi(0)/d\tau = L[(k + k_0)\beta_0 - k].$$

There are a large number of electrons spread randomly over each optical wavelength ($\sim 10^7$), so that the ξ_i can be accurately taken to be uniformly spread along each section of the electron beam one wavelength of light long. It can be easily seen in (1) that bunching the electrons near the relative phase $\xi + \phi \approx \pi$ drives the optical wave amplitude producing gain, while bunching near $\xi + \phi \approx \pi/2$ drives the optical phase ϕ without gain. Bunching electrons near $\xi + \phi \approx 0$ results in negative gain, or absorption. The dimensionless electron phase velocity v_i has an initial spread associated with the beam quality.

The electron motion in the presence of the optical wave is described by the Lorentz force equation: $d\gamma/dt = -(e/mc)\beta \cdot \mathbf{E}$. In the FEL, it is important to distinguish between collective Coulomb forces and collective high-gain effects.²⁶ Most FEL's do not use current densities large enough for Coulomb forces to be a significant effect for the relativistic electrons; yet, high gain is possible and will be included. Using the definitions and as-

sumptions above, the Lorentz force takes on the form of the pendulum equation,²⁷

$$\frac{d^2\xi}{d\tau^2} = \frac{dv}{d\tau} = |a| \cos(\xi + \phi). \quad (2)$$

The combined equations (1) and (2) are valid in weak or strong optical fields, for large or small gain, and for an arbitrary electron distribution. Strong fields near saturation mean that $|a| \gg \pi$, and weak fields occur when $|a| \ll \pi$. High gain is achieved when $j \gg 1$ and low gain occurs when $j \leq 1$.²⁸ Useful FEL configurations display a wide range of current densities. The electron-beam area is typically between 1 and 5 mm, but the current ranges from 1 A up to 10 kA. Undulator lengths L now range from 1 to 5 m, but will soon be made to $L = 20$ m and beyond. With electron energies in the range 10 MeV to 1 GeV, the corresponding values of j are from unity to more than 5×10^4 .¹ Both the high-gain, single-pass and the low-gain, oscillator configurations have important applications.

Equations (1) and (2) were originally derived²⁵ for the more general case where the electron energy can change significantly during a single pass; in this case, an additional factor $\eta = (1 - v/2\pi N)$ alters the wave and electron equations so that $\dot{a} = -j \langle \sqrt{\eta} e^{-i\xi} \rangle$ and,

$$\ddot{\xi} = \dot{v} = |a| \eta^2 \cos(\xi + \phi) \text{ with } (\dot{}) = d()/d\tau.$$

The following work, however, will be confined to weak optical fields where $\eta \approx 1$. An extension to higher harmonics and linearly polarized undulators is also possible without any change in form of (1) and (2), so that the general conclusions and methods of this paper are immediately applicable to a wide range of FEL designs.

We now proceed to solve (1) and (2) in weak fields, $|a| \ll \pi$, to obtain an integral equation for $a(\tau)$ incorporating an arbitrary electron distribution function. The electron phase can be expressed as $\xi = \xi_i + v_i\tau + \xi^{(1)}$ where $\xi^{(1)}$ is the first-order perturbation in a . Expanding (1) and (2) we have

$$\begin{aligned} a(\tau) &= a_0 + ij \int_0^\tau ds \langle \exp[-i(\xi_i + v_i s)] \xi^{(1)}(s) \rangle, \\ \xi^{(1)}(s) &= \frac{1}{2} \int_0^s dq \int_0^q du \{ a(u) \exp[i(\xi_i + v_i u)] \\ &\quad + a^*(u) \exp[-i(\xi_i + v_i u)] \}, \end{aligned} \quad (3)$$

where the initial optical field is $a(0) = |a(0)| = a_0$ and $\phi(0) = 0$. We have made use of

$$\langle \exp(-i\xi_i) \rangle = \int_0^{2\pi} d\xi_i \exp(-i\xi_i)/2\pi = 0,$$

since the initial electrons are spread uniformly in phase. The reference to the individual electron phases $\xi_i^{(1)}$ can be explicitly removed by combining the equations in (3). Then, we have an integral equation governing the evolution of the optical field $a(\tau)$:

$$a(\tau) = a_0 + \frac{ij}{2} \int_0^\tau ds \int_0^s dq \int_0^q du \langle \exp[-iv_i(s-u)] \rangle a(u), \quad (4)$$

where $\langle \dots \rangle$ is now an average over the initial electron velocity distribution, and all reference to the electron

phases has been removed. Since (4) is an iterated triple integral, it may be rewritten²⁹ as a double integral,

$$a(\tau) = a_0 + \frac{ij}{2} \int_0^\tau ds \int_0^s dq \langle \exp[-i\nu_i(s-q)] \rangle \times (s-q)a(q). \quad (5)$$

A normalized electron distribution function $f(\nu_i)$ can be used to evaluate the remaining average: $\langle \cdots \rangle \equiv \int_{-\infty}^{\infty} d\nu_i f(\nu_i) (\cdots)$ with $\int_{-\infty}^{\infty} d\nu_i f(\nu_i) = 1$.

III. SIMPLE ELECTRON DISTRIBUTIONS

We begin by considering two simple examples with perfect beam quality. In the first, we start the FEL on resonance where the electron-optical wave coupling is largest, $f(\nu_i) = \delta(\nu_i)$. The optical wave is most simply determined from (4):

$$a(\tau) = a_0 + \frac{ij}{2} \int_0^\tau ds \int_0^s dq \int_0^q du a(u). \quad (6)$$

The integral equation (6) can also be written in a differential form by taking successive derivatives, $\ddot{a}'(\tau) = ija(\tau)/2$. The complete solution uses the form $a(\tau) = \sum_{n=1}^3 a_n \exp(\alpha_n \tau)$ where the α_n are the three complex roots of the cubic equation $\alpha^3 - ij/2 = 0$, and the coefficients a_n are determined by the initial conditions $a(0) = a_0$ and $\dot{a}(0) = \ddot{a}(0) = 0$.¹ The solution for $a(\tau)$ is

$$a(\tau) = \frac{a_0}{3} \left\{ \exp[(j/2)^{1/3}(i + \sqrt{3})\tau/2] + \exp[(j/2)^{1/3}(i - \sqrt{3})\tau/2] + \exp[-i(j/2)^{1/3}\tau] \right\}. \quad (7)$$

If the current density is small $j \rightarrow 0$, or $\tau \ll 1$, we have the trivial result $a(\tau) = a_0(1 + ij\tau^3/12 + \cdots)$ for an FEL starting on resonance. There is no change in the optical amplitude $|a| = a_0 + \cdots$ to lowest order, and therefore no gain. The optical phase $\phi(\tau)$ increases slowly in proportion to τ^3 . The FEL gain is defined as $G(\tau) = [|a(\tau)|^2 - a_0^2]/a_0^2$, and

$$G(\tau) = \frac{1}{9} \left\{ 2 \cosh[(j/2)^{1/3}\sqrt{3}\tau] + 4 \cos[(j/2)^{1/3}3\tau/2] \times \cosh[(j/2)^{1/3}\sqrt{3}\tau/2] - 6 \right\}. \quad (8)$$

In the high-current limit, $j \gg 1$ on-resonance, the expressions simplify because one fastest growing root dominates and describes exponential growth in τ . As seen from (7) there is little change in the field during the bunching time, $\tau < \tau_B \approx (2/j)^{1/3}$, that precedes exponential growth. During this time, the electrons move from their initially uniform phase distribution to bunch near the phase $\zeta + \phi = \pi/2$. As soon as bunching forms, the high current immediately causes exponential field growth and high gain. Then,

$$a(\tau) \approx \frac{a_0}{3} \exp[(j/2)^{1/3}\sqrt{3}\tau/2],$$

and

$$G(\tau) \approx \frac{1}{9} \exp[(j/2)^{1/3}\sqrt{3}\tau]. \quad (9)$$

A second simple example is a high-quality electron beam starting off-resonance at ν_0 . This is characterized by $f(\nu_i) = \delta(\nu_i - \nu_0)$. The optical field is then determined by

$$a(\tau) = a_0 + \frac{ij}{2} \int_0^\tau ds \int_0^s dq \int_0^q du e^{-i\nu_0(s-u)} a(u). \quad (10)$$

For low current, $j \leq 1$, the optical field evolution away from a_0 is small so that $a(u) \approx a_0$ can be extracted from the integrand in (10). The resulting integrals are easily solved to obtain the usual low-current gain and phase-shift formulas.²⁷

$$G(\tau) = j \frac{2 - 2 \cos(\nu_0 \tau) - \nu_0 \tau \sin(\nu_0 \tau)}{\nu_0^3},$$

and

$$\phi(\tau) = j \frac{2 \sin(\nu_0 \tau) - \nu_0 \tau [1 + \cos(\nu_0 \tau)]}{2\nu_0^3}. \quad (11)$$

The maximum final gain is $G = 0.135j$ at $\nu_0 = 2.6$ and $\tau = 1$, while the range of modes with significant gain is $\delta\nu_0 \approx 1$ about the peak.

In order to obtain the general solution, use the substitution $b = ae^{i\nu_0 \tau}$ in (10). Successive derivatives then lead to the differential form of (10), $\ddot{b} - i\nu_0 \dot{b} - ib/2 = 0$. Solutions of the form $b = \sum_{n=1}^3 b_n \exp(\alpha_n \tau)$ have roots α_n that satisfy the cubic equation $\alpha_n^3 - i\nu_0 \alpha_n^2 - ib/2 = 0$. In the limit of high current $j \gg 1$, the exponential gain coefficient is reduced by the factor $-\nu_0^2/3\sqrt{3}(j/2)^{1/3}$ so that the gain spectrum is centered about $\nu_0 = 0$ with a characteristic range $\delta\nu_0 \approx 4.22j^{1/6}$. In the high-current case, the range of modes with significant gain increases slowly as j increases. We go on now to look at more interesting FEL distributions describing less than perfect electron beams.

IV. MORE GENERAL ELECTRON DISTRIBUTIONS

New cases of interest involve more complicated distributions $f(\nu_i)$ describing the initial electron beam in the integral equation (5). Two electrons starting at the same phase ζ_i at the beginning of the undulator ($\tau = 0$), but with different z velocities, $c\beta_0$ and $c(\beta_0 + \Delta\beta_0)$, will drift apart as they travel through the undulator. The amount of drift is not easily predicted without solving the full problem, because electrons can influence each other through the self-consistently evolving optical wave. In this sense, the effect of FEL beam quality is collective. However, the times for the two electrons to traverse the undulator are nearly identical since they are relativistic, $L/\beta_0 c \approx L/(\beta_0 + \Delta\beta_0)c \approx L/c$. An estimate of their separation at the end of the undulator ($\tau = 1$) is $\Delta z \approx \Delta\beta_0 L$, and their approximate phase difference is $\Delta\zeta = (k + k_0)\Delta z \approx k\Delta z \approx kL\Delta\beta_0$. If the velocity difference $\Delta\beta_0$ is due to an initial energy difference $\Delta\gamma mc^2$, we

have $\Delta\beta_0 \approx (1+K^2)\Delta\gamma/\gamma^3$, and an approximate final phase separation $\Delta\xi \approx 4\pi N\Delta\gamma/\gamma$.

Any random-phase difference $\Delta\xi \sim \pi$, or larger, between electrons in the beam is important to the FEL operation, because bunching on the optical wavelength scale is diminished significantly. At the end of the undulator, the final phase difference is roughly estimated by $\Delta\xi \approx \Delta v_i$ for each electron. From the definition of the electron phase velocity v_i , we see that a small change in the initial electron energy $\Delta\gamma mc^2$ corresponds to a change in the initial phase velocity, $\Delta v_i \approx 4\pi N\Delta\gamma/\gamma$ for $\gamma \gg 1$. A distribution of initial electron energies from an accelerator or storage ring is often accurately represented by the normal distribution function so that we can take

$$f(v_i) = \frac{\exp[-(v_i - v_0)^2/2\sigma^2]}{\sqrt{2\pi}\sigma}, \quad (12)$$

where σ is the standard deviation of v_i away from the peak phase velocity v_0 . If $\Delta\gamma mc^2$ is taken to be the standard deviation of the electron energy away from γmc^2 , then $\sigma \approx 4\pi N\Delta\gamma/\gamma$. Two electrons starting at the same phase ζ_i , but with an energy difference $\Delta\gamma = \gamma/4N$ will drift apart by roughly half of one optical wavelength at the end of the undulator. A random spread of width $\sigma = \pi$ causes a random-phase spread of approximately $\Delta\xi \approx \pi$ at the end of the undulator and impairs bunching. Inserting (12) into (5) gives

$$a(\tau) = a_0 + \frac{ij}{2} \int_0^\tau ds \int_0^s dq e^{-\sigma^2(s-q)^2/2} \times e^{-iv_0(s-q)}(s-q)a(q). \quad (13)$$

The Gaussian factor in the integrand decreases the coupling current j as τ increases, and describes the degradation of bunching due to the spread in electron phase velocities. The complicated self-consistent evolution of the electron-beam distribution and the optical field are described exactly in (13), but before evaluation, we can generalize its form further.

An angular spread is also possible due to the finite emittance of an electron beam. An electron of energy γmc^2 entering the undulator with a small injection angle θ_i has a reduced z velocity, $\beta_0 \rightarrow \beta_0 \cos\theta_i \approx \beta_0(1 - \theta_i^2/2)$. The resulting z velocity change is $\Delta\beta_0 \approx -\theta_i^2/2$, reducing the initial phase velocity by $\Delta v_i = -2\pi N\gamma^2\theta_i^2/(1+K^2)$. A Gaussian distribution of angles about the z axis with standard deviation $\Delta\theta_i$ gives the exponential distribution function

$$f(v_i) = \frac{\exp[-(v_0 - v_i)/\sigma_\theta]}{\sigma_\theta} \quad \text{for } v_i < v_0, \\ f(v_i) = 0 \quad \text{for } v_i > v_0, \quad (14)$$

where $\sigma_\theta = 4\pi N\gamma^2\Delta\theta_i^2/(1+K^2)$, and v_0 is the phase velocity for electrons entering on-axis. The distribution function (14) is sharply peaked at $v_i = v_0$ where electrons enter on-axis, and decays exponentially for $v_i < v_0$ because the injection at any angle θ_i can only decrease the electron's longitudinal velocity and its phase velocity v_i . If each element of the energy distribution (12) is given an

angular spread according to (14), then the resulting integral equation for the optical field becomes

$$a(\tau) = a_0 + \frac{ij}{2} \int_0^\tau ds \int_0^s dq \frac{e^{-\sigma^2(s-q)^2/2}}{1 - i\sigma_\theta(s-q)} \times e^{-iv_0(s-q)}(s-q)a(q). \quad (15)$$

The transverse motion of electrons injected at an angle is sometimes confined by either the natural off-axis undulator fields or external focusing elements. The focusing forces result in transverse betatron oscillations about the undulator axis. When the electron beam is injected to match the natural focusing properties of an undulator, the number of betatron oscillations along the undulator is $N_\beta \approx NK/\sqrt{2}\gamma$. In the limit of large γ and/or small K , the angular spread of electrons can be important, $\sigma_\theta > 1$, while the transverse focusing can be made negligible, $N_\beta < 1$. In this limit, the integral equation (15) applies.

The complex optical field $a(\tau)$ now depends on an input energy spread characterized by σ , and an input angular spread characterized by σ_θ . Other types of distribution functions can be added in a similar way. If (5) is solved numerically, even experimental distribution functions peculiar to a given accelerator or transport system can be added. The general result (5) and the specific example (15) are important results of this paper. They provide analytic expressions describing FEL performance with an arbitrary electron distribution function.

V. LOW-CURRENT FEL'S

One of the cases of general interest is the low-current FEL oscillator. Radiation energy is stored in an optical resonator, and repeatedly driven by successive electron pulses from an accelerator like a linac or storage ring. An important issue for the oscillator is the detrimental effect of the electron energy and angular distributions when the oscillator is starting from weak optical fields. In the low-current case, we can simplify (15) by taking $a(q) \approx a_0$ in the integrand of the integral equation, and neglecting higher-order terms in j . Without $a(q)$ in the integrand, the integral can be further simplified by noticing that $iqe^{-iv_0q} = -\partial_{v_0} e^{-iv_0q}$. Then,

$$\frac{a(\tau) - a_0}{a_0} = -\frac{j}{2} \frac{\partial}{\partial v_0} \int_0^\tau ds \int_0^s dq \frac{e^{-\sigma^2q^2/2}}{1 - i\sigma_\theta q} e^{-iv_0q}. \quad (16)$$

Direct integration of (16) is possible, but the result is a complicated expression containing many error functions.³⁰

We can alter the form of (16), however, to obtain some important physical interpretations. The factors $e^{-\sigma^2q^2/2}$ and $(1 - i\sigma_\theta q)^{-1}$ can be interpreted as power-series expansions in q multiplying the factor e^{-iv_0q} ; then $(-iq)^n e^{-iv_0q} \rightarrow \partial_{v_0}^n e^{-iv_0q}$. Now, write

$$\frac{a(\tau) - a_0}{a_0} = -\frac{j}{2} \frac{\exp(\sigma^2\partial_{v_0}^2/2)}{1 + \sigma_\theta\partial_{v_0}} \partial_{v_0} \int_0^\tau ds \int_0^s dq e^{-iv_0q}. \quad (17)$$

The double integral is simply $v_0^{-2}(1 - iv_0\tau - e^{-iv_0\tau})$, so that the complex integrations in (16) have been replaced with a power-series expansion to all orders in σ and σ_θ . To first order in σ and σ_θ , an explicit expression for $a(\tau)$ is easily obtained from (17). This is a useful limiting case since a low-current FEL system would not typically use a low-quality electron beam (large σ or σ_θ) and remain above threshold. From (17), the low-current FEL gain at the end of the undulator is

$$G = -\frac{j}{2} \frac{\exp(\sigma^2 \partial_{v_0}^2 / 2)}{1 + \sigma_\theta \partial_{v_0}} \partial_{v_0} \left[\frac{\sin^2(v_0/2)}{(v_0/2)^2} \right]. \quad (18)$$

We recognize the factor in square brackets [. . .] as the FEL spontaneous emission line shape for an electron in a perfect trajectory through the undulator. It has been known for some time that the gain is fundamentally related to the derivative of the spontaneous emission line shape.³¹ The new feature presented in (18) is to express how the electron-beam energy and angular spreads affect that relationship through successively higher derivatives.

With the physical interpretation of the line-shape factor [. . .], we can substitute alternate forms. One convenient choice is [. . .] $\rightarrow \exp(-v_0^2/4\pi)$ which approximately reproduces the correct features of the simple FEL gain spectrum, $G \approx (jv_0/4\pi)\exp(-v_0^2/4\pi)$. The successive derivatives evaluating the effects of beam quality lead to more compact expressions, and illustrate how (18) can be used in practical situations. Even an experimental line shape could be used in (18).

While the analytic results presented have their merit, the complete integral (15) is easy to integrate on a small computer. The values needed for the contour plots of this paper were evaluated in this way. Figure 1 shows a combined intensity and contour plot of $\ln[1 + G(\sigma, v_0)]$ where the final gain at the end of the FEL undulator is $G = [a^*(1)a(1) - a_0^2]/a_0^2$. In Fig. 1 $\sigma_\theta = 0$, so that gain degradation is only due to an energy spread with no angular spread. The current density is $j = 1$, and gives low gain

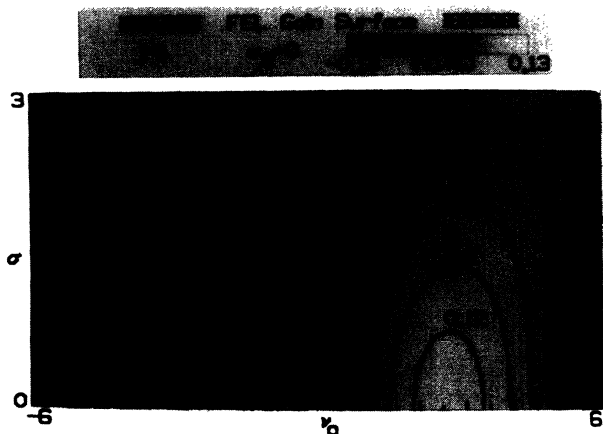


FIG. 1. Intensity and contour plot of $\ln[1 + G(\sigma, v_0)]$ with $j=1$ and $\sigma_\theta=0$. The weak-field gain degradation in this low-current FEL is due to an electron-beam energy spread with a normal distribution function.

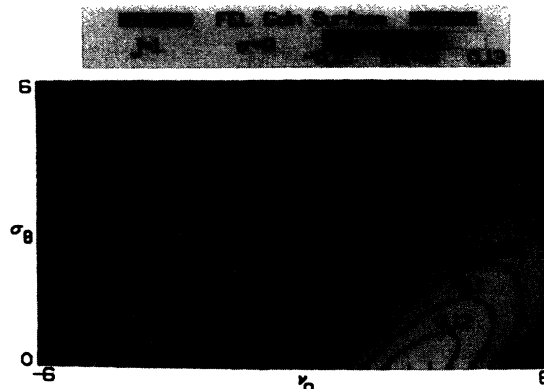


FIG. 2. Intensity and contour plot of $\ln[1 + G(\sigma_\theta, v_0)]$ with $j=1$ and $\sigma=0$. The weak-field gain degradation in this low-current FEL is due to an electron-beam angular spread with a normal distribution; the resultant phase-velocity distribution is the exponential distribution function.

so that $\ln(1 + G) \approx G$. The brightest points (white) on the (σ, v_0) surface indicate peak gain $G \approx 0.13j$, while the darkest points (black) indicate maximum absorption $G \approx -0.13j$. Zero gain is indicated by the intermediate grey shown in the scale at the top. Specific contours of constant gain, $\ln(1 + G) = \pm 0.06, \pm 0.08, \pm 0.1$, and ± 0.12 , are superimposed on the intensity plot. The gain surface is approximately antisymmetric about $v_0=0$, and in the limit $j \rightarrow 0$, the gain $G(\sigma, v_0)$ becomes exactly antisymmetric. The characteristic amount of spread required to decrease the gain is seen from Fig. 1 and (18) to be $\sigma^* \approx 1$. Note also that as the spread σ increases, the phase velocity for peak gain $v_0^* \approx 2.6$ increases slightly. Peak absorption occurs at $-v_0^*$ and slightly decreases with increasing σ .

Figure 2 shows a combined intensity and contour plot of $\ln[1 + G(\sigma_\theta, v_0)]$ evaluated by (15) with $j=1$ and $\sigma=0$. The gain degradation here is due to a monoenergetic electron beam entering the undulator with an angular spread described by σ_θ . The grey scale and contours of gain are the same as in Fig. 1. Unlike Fig. 1, the absorption contours (white) have a much different shape than the gain contours (black). Since the distribution function $f(v_i)$ due to an angular spread is skewed, there is no reason to expect the antisymmetric properties of $G(\sigma_\theta=0, v_0)$ to be maintained at $\sigma_\theta > 0$. As seen in Fig. 1 and (18), the characteristic value for the degradation of gain is $\sigma_\theta^* \approx 1$. The phase velocity for peak gain, and peak absorption, both increase with increasing σ_θ roughly as $v_0^* \approx \sigma_\theta$. Note that the general features of Figs. 1 and 2 are quite different owing to the different forms of the electron distributions. This emphasizes the importance of the shape of the electron distribution in evaluating gain degradation in FEL's, and the need for an accurate, flexible theory as presented here.

VI. HIGH-CURRENT FEL'S

The integral representation of the optical field in (15) is also valid for high-current FEL's where $j \gg 1$. In this case, $a(\tau)$ acquires a nonlinear dependence on j [recall ex-

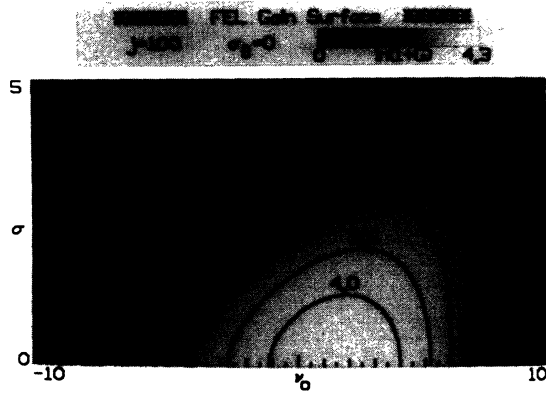


FIG. 3. Intensity and contour plot of $\ln[1 + G(\sigma, \nu_0)]$ with $j=100$ and $\sigma_\theta=0$. The weak-field gain degradation in this FEL is due to an electron beam with a normal distribution in energy.

pression (7)] and cannot be removed from the integral of (15). To proceed analytically, it is convenient to remove one integral from (15) by taking the τ derivative of both sides, and use the form $a = a_0 e^{\alpha\tau}$ for the optical field. Since $j \gg 1$, assume that α has some large real part, even though the exponential growth may be somewhat diminished by the presence of σ and σ_θ . The magnitude a_0 cancels on both sides, and a change of variables gives the form

$$\alpha^3 \approx \frac{ij}{2} \int_0^\infty ds s e^{-s} \frac{e^{-\sigma^2 s^2 / 2\alpha^2}}{1 - i\sigma_\theta s / \alpha} e^{-i\nu_0 s / \alpha}. \quad (19)$$

The upper integration limit in (19) has been extended to infinity because the integrand containing the factor e^{-s} becomes negligible for large s .

Equation (19) describes several properties of high-gain FEL's without integration. If σ , ν_0 , and σ_θ all go to 0, then α has the same roots found in (7). If the current density $j \rightarrow \infty$ so that a real part of $\alpha \rightarrow \infty$, then we obtain the same limit, since σ , ν_0 , and σ_θ all appear divided by α in (19). Unlike the low-current FEL, the importance of beam quality in a high-current FEL depends on the

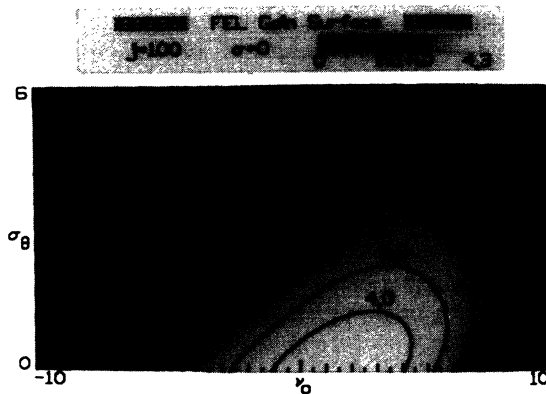


FIG. 4. Intensity and contour plot of $\ln[1 + G(\sigma_\theta, \nu_0)]$ with $j=100$ and $\sigma=0$. The weak-field gain degradation in this FEL is due to an electron beam with an angular spread producing an exponential distribution in phase velocities.

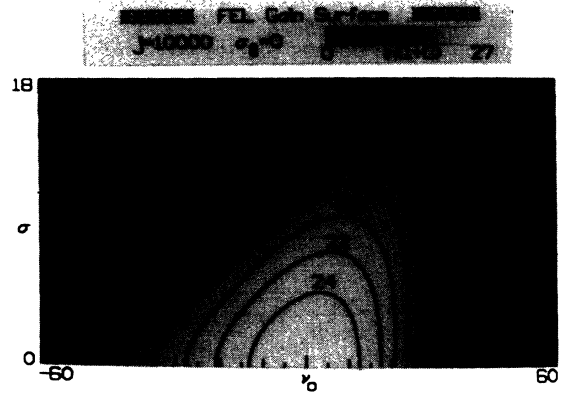


FIG. 5. Intensity and contour plot of $\ln[1 + G(\sigma, \nu_0)]$ with $j=10^4$ and $\sigma_\theta=0$. The weak-field gain degradation in this high-gain FEL is due to an electron beam with a normal distribution in energy.

current density j . This feature has been seen in FEL experiments and simulations, but is now expressed analytically. The importance of beam quality can be made more quantitative by iterating (19). Estimating the real part of the fast-growing root as $\alpha^* = (j/2)^{1/3} \sqrt{3}/2$, the integrand of (19) is only significantly modified when $\sigma^* \approx (j/2)^{1/3} \sqrt{3}/2$ or when $\sigma_\theta^* \approx (j/2)^{1/3} \sqrt{3}/2$. In the high-current FEL, the characteristic values of beam quality, σ^* and σ_θ^* , are not equal, and increase with the current density j . These expressions should be helpful in designing high-gain experiments where there is a trade-off between beam quality and beam current.

Figure 3 shows a combined intensity and contour plot of $\ln[1 + G(\sigma, \nu_0)]$ for moderately high current $j=100$ and $\sigma_\theta=0$. The points at the peak gain $\ln(1 + G)=4.3$ are indicated by white on the (σ, ν_0) surface; black indicates zero gain. Contours of constant gain, $\ln(1 + G) = 2.0, 2.5, 3.0, 3.5,$ and 4.0 are superimposed on the intensity plot. For the high-quality electron-beam, small σ , gain is confined to a region near resonance, but extends to a broader range in ν_0 than in the low-current cases of Figs. 1 or 2. This agrees with the discussion below (11),

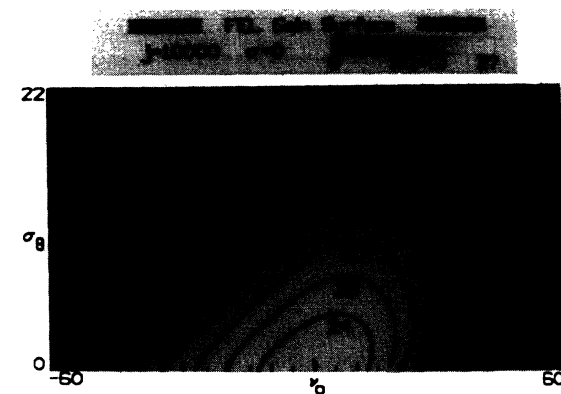


FIG. 6. Intensity and contour plot of $\ln[1 + G(\sigma_\theta, \nu_0)]$ with $j=10^4$ and $\sigma=0$. The weak-field gain degradation in this high-gain FEL is due to an electron beam with an angular spread producing an exponential distribution in phase velocities.

and gives the range of optical wavelengths over which there is significant gain $\delta\nu_0 \approx 4j^{1/6} \approx 7$. To find the range of wavelengths, use $\Delta\lambda/\lambda \approx \Delta\nu_0/2\pi N$ about the resonant wavelength $\lambda = \lambda_0(1 + K^2)/2\gamma^2$. The maximum available gain decreases significantly as $\sigma \rightarrow \sigma^* \approx 4.5$ as predicted in the previous paragraph, and the phase velocity for peak gain roughly follows $\nu_0^* \approx \sigma$.

Figure 4 shows the plot of $\ln[1 + G(\sigma_\theta, \nu_0)]$ with $\sigma = 0$ so that the gain degradation is caused by an angular spread in the electron beam. The contours of constant gain differ from Fig. 3 because of the new shape of the electron distribution function. As σ_θ increases, there is a slower decrease in gain because $\sigma_\theta^* > \sigma^*$ as found above. When expressed in dimensionless form, an angular spread is better tolerated in an FEL than is an energy spread. The points of peak gain increase with increasing σ_θ similar to Fig. 3.

Figure 5 shows the combined intensity and contour plot of $\ln[1 + G(\sigma, \nu_0)]$ for high current $j = 10^4$ with $\sigma_\theta = 0$. There are no negative gain regions, and the available peak gain is much larger than for the lower current. For $\sigma \approx 0$, the position of peak gain is essentially at resonance $\nu_0 = 0$, but again increases roughly as $\nu_0^* \approx \sigma$ while beam quality diminishes. The width of the gain spectrum at $\sigma = 0$ is

wider than the lower current case, and agrees well with $\delta\nu_0 \approx 4j^{1/6} \approx 12$. The contours of constant gain, $\ln(1 + G) = 14, \dots, 24$, show that the range of wavelengths for gain becomes narrower as σ increases, and the maximum available gain decreases significantly as $\sigma \rightarrow \sigma^* \approx 20$.

Figure 6 shows the plot of $\ln[1 + G(\sigma_\theta, \nu_0)]$ for high current $j = 10^4$ with $\sigma = 0$. Again, the contours of constant gain, $\ln(1 + G) = 14, \dots, 24$, are distinct from Fig. 5 showing the importance of the electron-beam distribution function even at high gain. As $\sigma_\theta \rightarrow \sigma_\theta^*$, the gain decreases significantly, but again the angular spread is seen to be less harmful than an energy spread. Unlike Fig. 5, the position of peak gain stays closer to resonance as σ_θ increases.

ACKNOWLEDGMENTS

The authors are grateful for support of this research by the U.S. Office of Naval Research, the Los Alamos National Laboratory, the Naval Research Laboratory, and the Lawrence Berkeley Laboratory, and would like to thank S. W. McDonald for helpful discussions.

¹W. B. Colson and A. M. Sessler, *Annu. Rev. Nucl. Part. Sci.* **35**, 25 (1985).
²S. Benson, D. A. G. Deacon, J. N. Eckstein, J. M. J. Madey, K. Robinson, T. I. Smith, and R. Taber, *J. Phys. (Paris) Colloq.* **44**, C1-353 (1983).
³J. A. Edighoffer, G. R. Neil, C. E. Hess, T. I. Smith, S. W. Fornaca, and H. A. Schwettman, *Phys. Rev. Lett.* **52**, 344 (1984).
⁴M. Billardon *et al.*, *Phys. Rev. Lett.* **51**, 1652 (1983).
⁵L. R. Elias, J. Hu, and G. Ramian, *Nucl. Instrum. Math. Phys. Res.* **A237**, 203 (1985).
⁶*Free Electron Generation of Extreme Ultraviolet Coherent Radiation, Brookhaven National Laboratory, 1983*, edited by J. M. J. Madey and C. Pellegrini (AIP, New York, 1984).
⁷V. K. Neil, JASON Technical Report JSR-79-10, SRI International, 1979 (unpublished).
⁸Ira B. Bernstein and J. L. Hirshfield, *Phys. Rev. Lett.* **40**, 761 (1978).
⁹Ira B. Bernstein and J. L. Hirshfield, *Phys. Rev. A* **20**, 1661 (1979).
¹⁰N. M. Kroll and W. A. McMullin, *Phys. Rev. A* **17**, 300 (1978).
¹¹P. Sprangle, Cha-Mei Tang, and W. M. Manheimer, *Phys. Rev. A* **21**, 302 (1980).
¹²P. Sprangle and Robert A. Smith, *Phys. Rev. A* **21**, 293 (1980).
¹³W. B. Colson and S. K. Ride, *Physics of Quantum Electronics*, edited by S. Jacobs, H. Pilloff, M. Sargent, M. O. Scully, and R. Spitzer (Addison-Wesley, Reading, Mass., 1980), Vol. 7, p. 377.
¹⁴F. Ciocci, G. Dattoli and A. Renieri, *Lett. Nuovo Cimento* **34**, 342 (1982).
¹⁵I. Boscolo, M. Leo, R. A. Leo, and G. Soliani, *Nuovo Cimento* **2D**, 64 (1983).
¹⁶J. C. Goldstein, W. B. Colson, and R. W. Warren, *Bendor*

Free Electron Laser Conference [*J. Phys. (Paris) Colloq.* **44**, C1-371 (1983)].
¹⁷L. F. Ibenez and S. Johnston, *IEEE J. Quantum Electron.* **QE-19**, 339 (1983).
¹⁸J. Gea-Banacloche, G. T. Moore, and M. O. Scully, *Free Electron Generators of Coherent Radiation* (Society of Photo-Optical Instrumentation Engineers, Bellingham, WA, 1983), p. 393.
¹⁹J. Gea-Banacloche, G. T. Moore, and M. O. Scully, in *Free Electron Generation of Extreme Ultraviolet Coherent Radiation, Brookhaven National Laboratory, 1983*, edited by J. M. J. Madey and C. Pellegrini (AIP, New York, 1984) p. 161.
²⁰G. T. Moore, *Opt. Commun.* **54**, 121 (1985).
²¹L. K. Grover, J. Feinstein, R. H. Pantell, *IEEE J. Quantum Electron.* **QE-21**, 470 (1985).
²²K.-J. Kim, *Nucl. Instrum. Methods A* **250**, 396 (1986).
²³G. Dattoli and A. Renieri, in *Experimental and Theoretical Aspects of the Free Electron Laser*, Vol. 4 of *Laser Handbook*, edited by M. L. Stich and M. S. Bass (North-Holland, Amsterdam, 1985).
²⁴E. Jerby and A. Gover, *IEEE J. Quantum Electron.* **QE-21**, 1041 (1985).
²⁵W. B. Colson and S. K. Ride, *Phys. Lett.* **76A**, 379 (1980).
²⁶W. B. Colson, *IEEE J. Quantum Electron.* **QE-17**, 1417 (1981).
²⁷W. B. Colson, *Phys. Lett.* **A64**, 190 (1977).
²⁸W. B. Colson and R. A. Freedman, *Phys. Rev. A* **27**, 1399 (1983).
²⁹*Handbook of Mathematical Functions*, edited by M. Abramowitz and I. A. Stegun (U.S. GPO, Washington, D.C., 1972), p. 891.
³⁰P. M. Bosco, Ph.D. thesis, University of California at Santa Barbara, 1985.
³¹J. M. J. Madey, *J. Appl. Phys.* **42**, 1906 (1971).

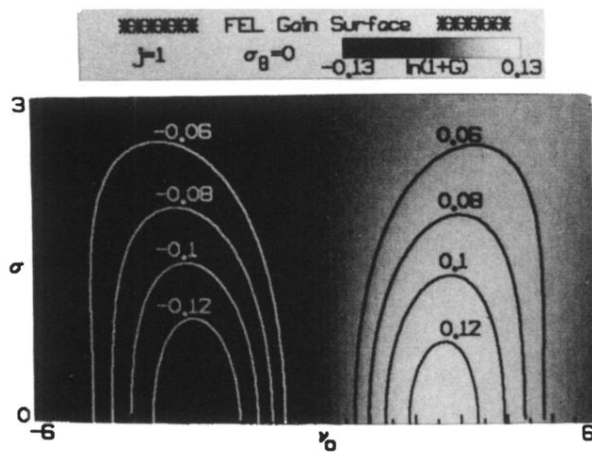


FIG. 1. Intensity and contour plot of $\ln[1 + G(\sigma, \nu_0)]$ with $j=1$ and $\sigma_\theta=0$. The weak-field gain degradation in this low-current FEL is due to an electron-beam energy spread with a normal distribution function.

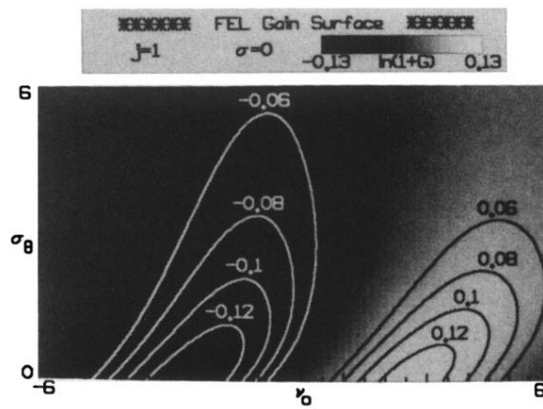


FIG. 2. Intensity and contour plot of $\ln[1 + G(\sigma_\theta, v_0)]$ with $j=1$ and $\sigma=0$. The weak-field gain degradation in this low-current FEL is due to an electron-beam angular spread with a normal distribution; the resultant phase-velocity distribution is the exponential distribution function.

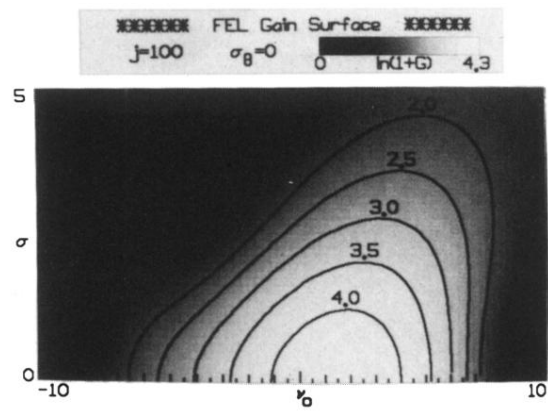


FIG. 3. Intensity and contour plot of $\ln[1 + G(\sigma, \nu_0)]$ with $j=100$ and $\sigma_\theta=0$. The weak-field gain degradation in this FEL is due to an electron beam with a normal distribution in energy.

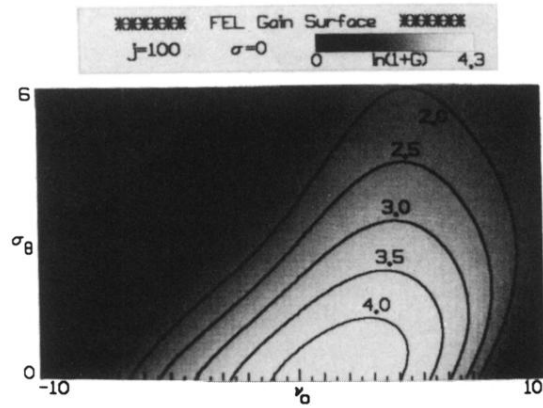


FIG. 4. Intensity and contour plot of $\ln[1 + G(\sigma_\theta, \nu_0)]$ with $j=100$ and $\sigma=0$. The weak-field gain degradation in this FEL is due to an electron beam with an angular spread producing an exponential distribution in phase velocities.

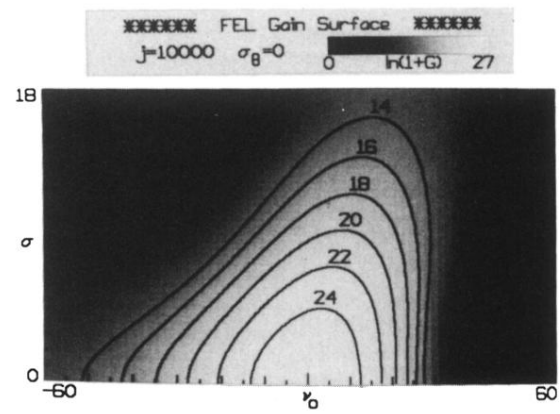


FIG. 5. Intensity and contour plot of $\ln[1 + G(\sigma, \nu_0)]$ with $j=10^4$ and $\sigma_\theta=0$. The weak-field gain degradation in this high-gain FEL is due to an electron beam with a normal distribution in energy.

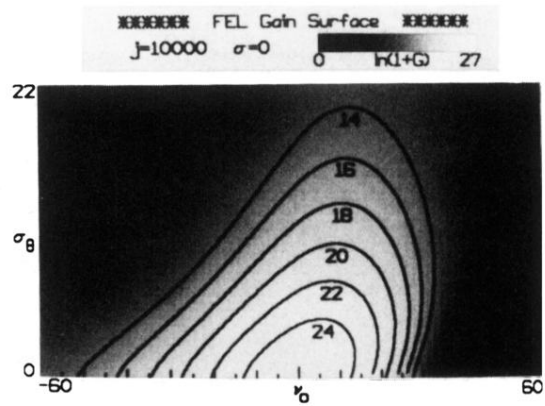


FIG. 6. Intensity and contour plot of $\ln[1 + G(\sigma_\theta, \nu_0)]$ with $j=10^4$ and $\sigma=0$. The weak-field gain degradation in this high-gain FEL is due to an electron beam with an angular spread producing an exponential distribution in phase velocities.